2010 E-Defense Four-Story Reinforced Concrete and Post-Tensioned Buildings – Preliminary Comparative Study of Experimental and Analytical Results

Z. Tuna, S. Gavridou, J. W. Wallace
University of California, Los Angeles, USA

T. Nagae and T. Matsumori
National Research Institute for Earth Science and Disaster Prevention, Japan

SUMMARY:
A series of shaking table tests were conducted on two, full-scale, four-story buildings on the NIED E-Defense shake table in December 2010. The buildings were almost identical in geometry and configuration; one building utilized a conventional reinforced concrete (RC) structural system with shear walls in one direction and moment frames in the other direction, whereas the other building utilized the same systems constructed with post-tensioned (PT) members. The buildings were simultaneously subjected to increasing intensity shaking until large deformations were reached to assess performance in service, design, and maximum considered earthquake shaking. Nonlinear response history analyses were conducted for the shear wall direction of the two buildings using CSI Perform3D in order to compare analytical and experimental results. Although the analytical models captured global response parameters reasonably well for the service- and design-level events, some inconsistencies between the simulated and measured responses were noted in the collapse-level event.

Keywords: shake table, reinforced concrete, shear wall, unbounded post-tensioned wall, nonlinear modeling

1. INTRODUCTION

The 2010 NIED E-Defense tests included testing of two buildings, a conventional reinforced concrete (RC) building, and a high-performance post-tensioned (PT) building. The two buildings were similar in geometry and configuration, with shear walls in one principle direction, and moment frames in the other direction. The buildings were subjected to increasing intensity shaking using the Kobe and Takatori records until large deformations were reached. The conventional RC building was designed according to the Japanese Standard Law (2007) and Architectural Institute of Japan requirements (AIJ, 1999), and also satisfied a majority of ASCE/SEI 7-05 and ACI 318-08 requirements for Special RC Structural Walls and Special RC moment frames (with an exception of strong column-weak beam requirements). The PT building was designed using a performance-based seismic design methodology and included high performance, post-tensioned lateral force-resisting systems. Moment frames consisted of precast prestressed beam and column elements, whereas structural walls utilized unbonded post-tensioned and mild steel to provide re-centering and energy dissipation characteristics. In addition, the PT building incorporated high performance materials such as high-strength concrete with steel fibers and high-strength transverse reinforcement. To meet the various design objectives, the base shear design strength of the PT building ended up being about twice that of the RC building in both directions.

This study focuses on providing comparisons between measured and predicted (analytical) responses for the shear wall direction of the two buildings. Although use of relatively complex nonlinear modeling approaches have become common for design of shear wall buildings (e.g., PEER/ATC 72-1, 2010), field and laboratory data for full-scale buildings subjected to multi-axis shaking are lacking to assess the reliability of these models. Experimental data are mostly available for two-dimensional, moderate-scale structures tested under quasi-static loading (e.g. Birely et al., 2010; Tran et al. 2011), and relatively limited buildings systems tested under uniaxial motions on shaking tables (Panagiotou al., 2008). This is especially true for unbonded post-tensioned wall systems. Therefore, the full-scale, three dimensional, dynamic tests on the NIED E-Defense shaking table provide information to fill an important knowledge gap as well as a wealth of data to assess the ability of both simple and complex nonlinear modeling approaches to reliably predict important global and local responses, including system interactions. This paper presents results obtained from nonlinear response history analyses of the RC and PT buildings along with comparisons with experimentally measured data. The models were developed using Perform 3D (CSI, 2011) because this software is commonly used in engineering practice in the United States, and similar programs are used worldwide. Preliminary results for a range of responses are compared including roof drifts, inter-story drifts, base overturning moments, floor accelerations, base wall rotations, and wall shear deformations. The test program, analytical models, and the ability of the analytical models to capture the measured responses are discussed in the following sections. Detailed information about the test program, including information about instrumentation and ground (table) motions is provided in PEER Report 2011/104 (Nagae et al., 2011).

2. DESCRIPTION OF THE TEST

The E-Defense shake table, the largest in the world, has plan dimensions of 20 m × 15 m allowing the two buildings to be tested simultaneously as shown in Figure 1(a). Each building weighed approximately 5900 kN and the combined weight of the two buildings was 98% of E-Defense table capacity. Descriptions of the RC and PT buildings are summarized in the following subsections.

Figure 1. (a) Overview of the test buildings; (b), (c) instrumentation of the RC shear wall

2.1. Test buildings

The lateral-force-resisting systems for the test buildings consisted of two-bay moment frames in the longitudinal-direction (x) and two structural walls, one at each end of the building plan, in the transverse-direction (y) (Figure 2). Story heights at all levels for both buildings were 3 m, producing a building with an overall height of 12 m. Floor plan dimensions were 14.4 m (x) and 7.2 m (y).

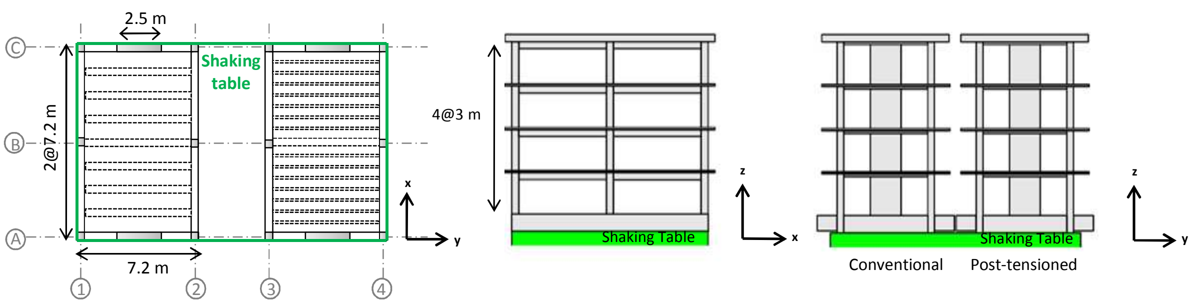

Figure 2. Plan and elevation views of the test specimens

2.1.1. RC Building – Wall Direction

Member cross-section dimensions were 500 mm × 500 mm for columns, 250 mm × 2500 mm for walls, 300 mm × 400 mm for interior beams at Axis B, and 300 mm × 300 mm for beams at axes A and C. Additional beams with cross sections of 300 × 400 mm supported the floor slab at intervals of

1.5 m. A 130 mm-thick floor slab was used at floor levels 2 through 4 and at the roof level. The design concrete compressive strength was 27 N/mm2. Primary longitudinal reinforcement consisted of 19 mm and 22 mm diameter bars. The actual material properties of concrete and steel used in the test buildings are presented in Table 1. Reinforcement details of shear walls are presented in Figure 3. It is noted that transverse reinforcement was different in the North (Axis A) and South (Axis C) walls.

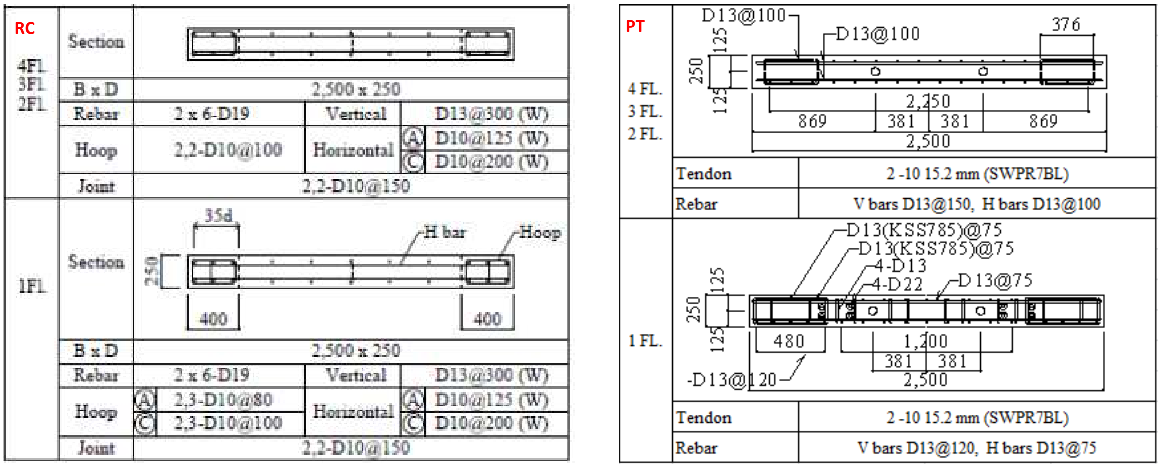

Figure 3. Cross-sections of the shear walls

Table 1. Actual material properties

RC Building

Steel	Grade	A_{normal} (mm^2)	σ_y (MPa)	σ_t (MPa)
D22	SD345	387	370	555
D19	SD345	287	380	563
D13	SD295	127	372	522
D10	SD295	71	388	513

Concrete	F_c (MPa)	σ_y (MPa)	Age (Days)
1st-2nd floor	27	39.6	91
2nd-3nd floor	27	39.2	79
3rd-4th floor	27	30.2	65
4th-roof floor	27	41.0	53

PT Building

Steel	A_{normal} (mm^2)	σ_y (MPa)	σ_t (MPa)
D22 (ED wall base)	387	385	563
PT bar φ21 (column)	346.4	1198	1281

	A_{normal} (mm^2)	F_y (kN)	F_t (kN)
PT wire φ15.2	140.7	250	277
PT wire φ17.8 (beam)	208.4	356	404

Concrete	F_c (MPa)	σ_y (MPa)
Precast concrete (normal)	60	83.2
Precast concrete (fiber)	60	85.5

2.1.2. PT Building

In the PT building, member cross sections consisted of 450 mm x 450 mm columns, 250 mm x 2500 mm walls, and 300 mm x 300 mm beams. Column PT tendons were grouted while the tendons located in walls and beams were unbonded (sheathed and greased) from anchor to anchor. PT tendons were stressed to 60% of the yield stress for the walls and exterior beams in the y-direction, and 80% of the yield stress for all other prestressed members. Walls were constructed of four precast concrete panels with eight D22 mild steel bars, unbonded over a length of 1.5m across the foundation-wall interface, to provide energy dissipation for the Unbonded, Post-Tensioned (UPT) wall. The design concrete compressive strength for the PT building was 60 N/mm^2. High-performance fiber reinforced cement composite was used at the first and second story wall panels of the North wall, while conventional concrete mix was used for the remaining wall panels. The actual concrete and steel properties are presented in Table 1 whereas reinforcement details of the UPT walls are shown in Figure 3.

2.2. Test plan, Ground (Table) Motions, and Instrumentation

The test buildings were subjected to the JMA-Kobe motions recorded in 1995, scaled by 25%, 50%, and 100%, to produce a range of shaking intensities. At the completion of these tests, two additional tests were conducted using the JR-Takatori record scaled by 40% and 60%. Pseudo acceleration and displacement spectra of the Kobe ground motions are presented in Figure 4(a) and 4(b), respectively, along with spectra for a service level (SLE; 50% in 30 years), design level (DBE; 10% in 50 years), and maximum considered earthquake level (MCE; 2% in 50 years) based on ASCE 7-10 requirements (ASCE, 2010) assuming that the buildings were located in downtown Los Angeles for Site Class B. Peak spectral accelerations observed on the shaking table were 0.89g, 1.58g and 3.42g at 25%, 50% and 100% Kobe records, respectively. It is noted that spectral acceleration demands for the 25% Kobe record are close to the SLE spectrum. For the 50% Kobe record, the demands are bounded by the DBE and MCE spectra near building fundamental periods (approximately 0.3 sec for both buildings), whereas the demands for the 100% Kobe record were much higher than the MCE spectrum.

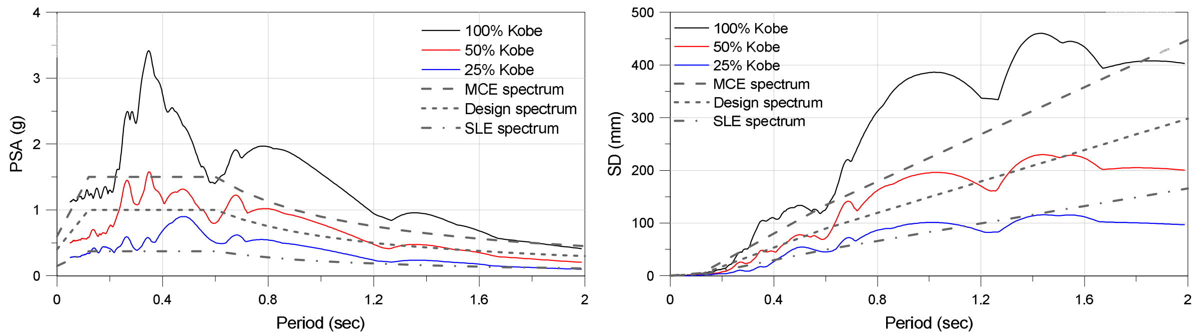

Figure 4. (a) Acceleration spectra, (b) Displacement spectra of the Kobe records

The two test buildings were heavily instrumented to enable performance assessment and post-test analytical studies. A total of 609 channels of data were collected during the tests for RC and PT specimens, including accelerometers, displacement transducers (wire potentiometers, laser-type displacement transducers, and linear variable differential transducers (LVDTs)), and strain gauges. Typical instrumentation of the shear walls are shown in Figure 1(b) and (c).

3. TEST RESULTS

Preliminary findings are presented in the following for the RC and PT buildings for the Kobe records.

3.1. RC Building

Figure 5(a) shows the roof drift histories of the RC building. Peak roof drifts are 0.2% (δ=23.5 mm), 0.84% (δ=100.7 mm), and 2.54% (δ=304.2mm) for 25%, 50% and 100% Kobe records, respectively. Residual roof level displacement of 21 mm (0.2% drift) is noted for the 100% Kobe record. Figure 6a presents the building overturning moment versus roof drift relations, with base moment calculated as floor masses times absolute floor accelerations, multiplied by the associated floor heights from the base. Results presented in Figure 6(a) indicate essentially elastic response for the 25% Kobe record and some inelastic response (yielding, along with modest stiffness and strength degradation) for the 50% Kobe record. Significant yielding and stiffness degradation, along with modest strength degradation, are noted for the 100% Kobe record. Based on test observations, strength loss was likely due to concrete crushing and reinforcement buckling at wall boundaries (Figure 7(a)). Following crushing of concrete at the wall boundaries, substantial sliding was observed at the wall base for the 50% and 100% Kobe records.

3.2. PT Building

Figure 5(b) presents the roof drift time histories for the PT building. Peak roof drifts are 0.15% (δ=17.5mm), 0.46% (δ=54.9mm) and 1.38% (δ=165.9mm) for 25%, 50% and 100% Kobe records, respectively. Complete self-centering response (zero residual displacements at the end of the record) was achieved for all three tests. Peak drift values for the PT building were generally less than those measured for the RC building. Figure 6(b) presents the building overturning moment versus roof drift relations for the PT building. For the 25% Kobe record, responses are nearly elastic without significant energy dissipation or softening. For the 50% Kobe record, minor energy dissipation (associated with yielding of the mild steel reinforcement) and softening behavior (associated with gap opening at the base joint) are observed. For the 100% Kobe record, significant hysteretic energy dissipation and stiffness degradation are observed. Minor damage occurred only at the wall-foundation interface and was limited to concrete spalling at wall toes (Figure 7(b)).

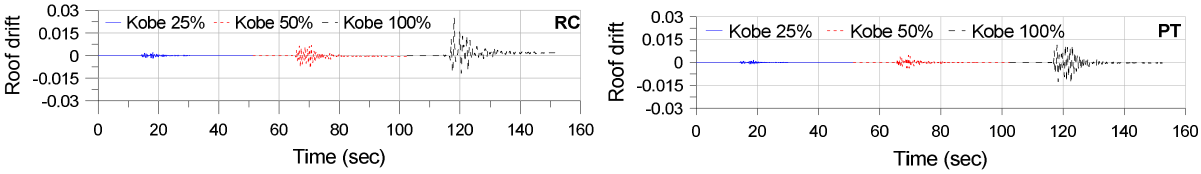

Figure 5. Roof drift histories of (a) RC building, (b) PT building

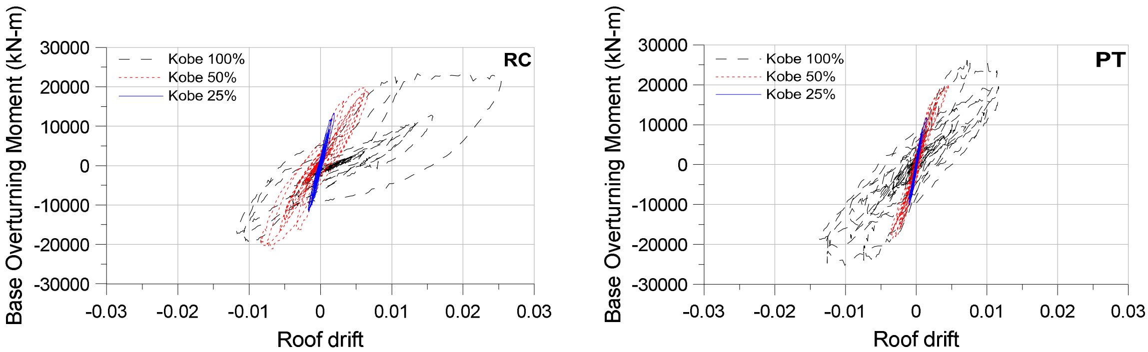

Figure 6. Base moment vs. roof drift outputs of (a) RC building, (b) PT building

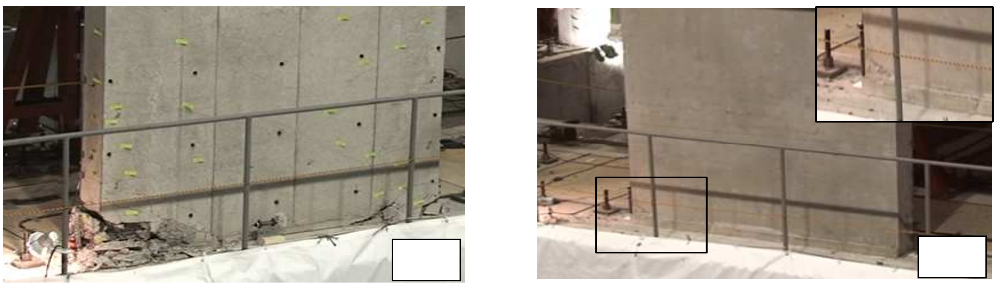

Figure 7. Damage on the (a) RC (Axis A) and (b) PT (Axis A) shear walls under 100% Kobe record

4. PRELIMINARY MODELING AND RESULTS

Preliminary analytical models for the shear wall directions of RC and PT buildings (axes A, B and C in Figure 2) were developed using Perform 3D. These models represent "blind" predictions without taking advantage of information gleaned from test data. For the RC building, the model was based on current modeling techniques (Tuna, 2009) and recommendations provided by PEER/ATC Report 72 (2010). For the PT building, the Unbonded Post-Tensioned (UPT) wall was modeled based on recommendations by Kurama et al., 1999 and Perez et al. 2004. Three-dimensional and elevation views of the RC and PT models are shown in Figure 8. The models consist of shear walls with fiber cross sections and frame elements for beams and columns. Additional information on the modeling of each building is described in the following subsections.

4.1. RC Modeling

4.1.1. Shear wall modeling

Shear walls were modeled using 4-noded, uniaxial, fiber "Shear Wall Elements". Plane sections are assumed to remain plane after loading and uniaxial material models for concrete and reinforcement are used to determine section and element responses. Unconfined concrete was modeled using a stress-strain relation based on the results of material characterization tests that were performed prior to the shake table testing (Nagae et al., 2011). The stress-strain relations of the reinforcement were defined using trilinear relationships based on the test results (Table 1). Shear behavior was modeled using a trilinear relation similar to that recommended by ASCE 41-06 Supplement #1. The uncracked shear modulus was taken as $G_c = E_c 2(1+\nu) \approx 0.4E_c$ and shear cracking was assumed to occur at $0.25\sqrt{f_c^{'}}MPa\ \left(3\sqrt{f_c^{'}}psi\right)$, but not greater than $0.5V_n$, where V_n is the ACI 318-08 nominal wall shear strength. The post-cracking slope was taken as $0.01E_c$ to account for nonlinear shear deformations due to shear-flexure interaction (Massone et al, 2006; PEER/ATC 72-1, 2010).

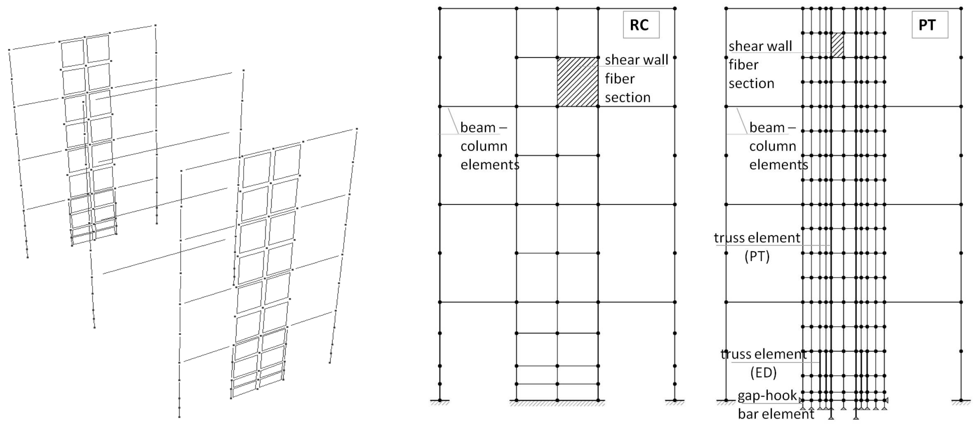

Figure 8. Three-dimensional and elevation views of the RC model and the PT model

4.1.2. Beam and column modeling

Beams and columns were defined as elastic beam-column elements with rigid end zones and plastic hinges at member ends. Elastic element effective stiffness of $0.3EI_g$ was used for both beams and columns as recommended in ASCE 41-06. Beam moment-rotation hinges were modeled using tri-linear backbone curves, whereas for the column plastic hinges, moment-axial capacity interaction curves were calculated using actual material properties. Cyclic degradation and strength loss were neglected in both beam and column hinges in the preliminary model.

4.2. PT Modeling

4.2.1. Shear wall modeling

The UPT shear walls in the PT building were modeled as described in Sec. 4.1.1 with modifications to capture the gap-opening behavior at the wall-foundation interface and to account for the different material properties. The confined concrete stress-strain relationship was defined based on the Razvi and Saatcioglu (1999) model. Elastic shear behavior was defined since the majority of lateral displacements in UPT walls is attributed to rocking at the wall-foundation interface and the contributions of wall shear (and flexural) deformations are expected to be small (Holden et al., 2003). The unbonded PT steel and the unbonded length of the energy dissipating bars were implemented as inelastic (truss) bar elements, placed outside of the fiber section as strain compatibility is not enforced between concrete and steel over the unbonded lengths. A tri-linear force-deformation relationship that approximates the actual stress-strain relation of the PT and mild steel was assigned to the truss elements. The prestressing force was simulated as an element load (initial strain) in the PT bar element. The gap-opening behavior at the base of the wall was modeled using elastic gap-hook bar elements with no tension strength; therefore, they act like compression-only springs and allow uplift in tension.

4.2.2. Beam and column modeling
In the PT building, beam mild reinforcement does not cross the beam-joint interface; therefore, no hystereric energy dissipation ocurrs at the beam-joint interface and moment capacity is provided only by unbonded post-tensioning steel. This connection allows a gap to open and close at the beam-column interface producing a nonlinear elastic moment-rotation behavior (provided that the PT steel does not yield). Initial analyses for the 50% and 100% records assuming linear elastic behavior and gross-section properties for the prestressed beams and columns resulted in beam moment demands that exceeded the yield moment, indicating that nonlinear behavior (softening associated with gap opening) should be considered. It is noted that the moment capacity of the beams was estimated using section analysis for UPT precast members proposed by Pampanin et al. (2001). For this preliminary study, the nonlinear behavior at the beam-column joint interface was modeled using beam moment-rotation hinges with elastoplastic behavior and large cyclic (energy) degradation factors (Perform 3D does not contain a nonlinear elastic rotational spring within its component library).

4.3. Damping and masses

Rayleigh damping of 2.5% at $0.2T_1$ and $1.0T_1$, where T_1 is the calculated first mode period, were used for the nonlinear response history analyses based on the recommendation of PEER/ATC Report 72 (2010). The seismic masses, lumped at center of the wall at each floor level, were based on the weight of the structures reported by Nagae et al. (2011). Axial load ratios at the base of the walls were estimated to be about $0.04A_gf'_c$ and $0.01A_gf'_c$ for the RC and PT buildings, respectively.

4.4. Comparisons of the preliminary analytical results with test results

Figure 9 displays comparisons of the preliminary analytical results with test results for the RC and the PT models in terms of base moment vs. roof drift for the 25%, 50%, and 100% Kobe records. Note that only the global responses are presented here due to space limitations.

Figure 9(a) indicates that the preliminary model is capable of capturing global responses and initial stiffness of the RC building for the 25% Kobe record, which is essentially elastic; whereas for the 50% Kobe (Figure 9(b)) and 100% Kobe (Figure 9(c)) records, stiffness degradation is not captured, and displacements and forces determined with the analytical model are generally underestimated, i.e., the model is too stiff. Potential factors that could lead to model results underestimating roof displacements of the test building include: (i) stiffness reduction due to slip/extension deformations at beam-joint and column-joint interfaces are underestimated (e.g., see Elwood et al, 2007; Naish, 2010), and (ii) deformations associated with sliding at the wall base are neglected (and test observations indicate modest sliding occurred for the 50% Kobe record, and significant sliding displacements were measured for the 100% Kobe record). Additional factors that might impact model results include (iii) cyclic degradation, and (iv) tension strength of concrete, which were neglected in the initial model. The preliminary model was modified to address the potential influence of each of these factors.

Figure 9(d) indicates that the analytical model for the PT building appears to satisfactorily predict the initial stiffness of the building. The model also provides a good estimate of the hysteretic response under the 50% Kobe record (Figure 9(e)). In particular, stiffness, strength and peak displacements are reasonably well predicted. However, it is observed that the number of large excursions in the positive direction is underestimated. Finally, for the 100% Kobe record (Figure 9(f)), peak displacements are accurately predicted but the model does not capture the softening and stiffness degradation that is apparent in the test results, and energy dissipation is underestimated. Additional studies are being conducted to improve the model and to more accurately incorporate the gap-opening behavior at the beam-column and beam-wall connections, e.g., by using inelastic fiber sections for beams and columns. Fiber models for UPT beam-to-column connections have been shown to provide good estimates of the hystretic response of these systems and have been previously validated with experimental data (El Sheik et al., 1999). Implementation of the model using a different software program that allows definition of nonlinear elastic rotational springs (e.g. OpenSees, RUAUMOKO (Carr, 2010)) for the UPT connections will also be considered (i.e., lumped plasticity models). Another issue that will be examined is the damping mechanism associated with impact at the wall-foundation interface. In the preliminary analyses, 2.5% Rayleigh damping was used (consistent with the RC model). Ma et al. (2006) identified energy dissipating mechanisms associated with impact at the rocking interface as the primary challenge in modelling the dynamic response of unbonded post-tensioned walls and emphasize that viscous damping should not be used to model energy loss due to impacts. Sensitivity of the analytical results to different values of viscous damping will be examined and implementing contact elements at the base of the wall also will be considered.

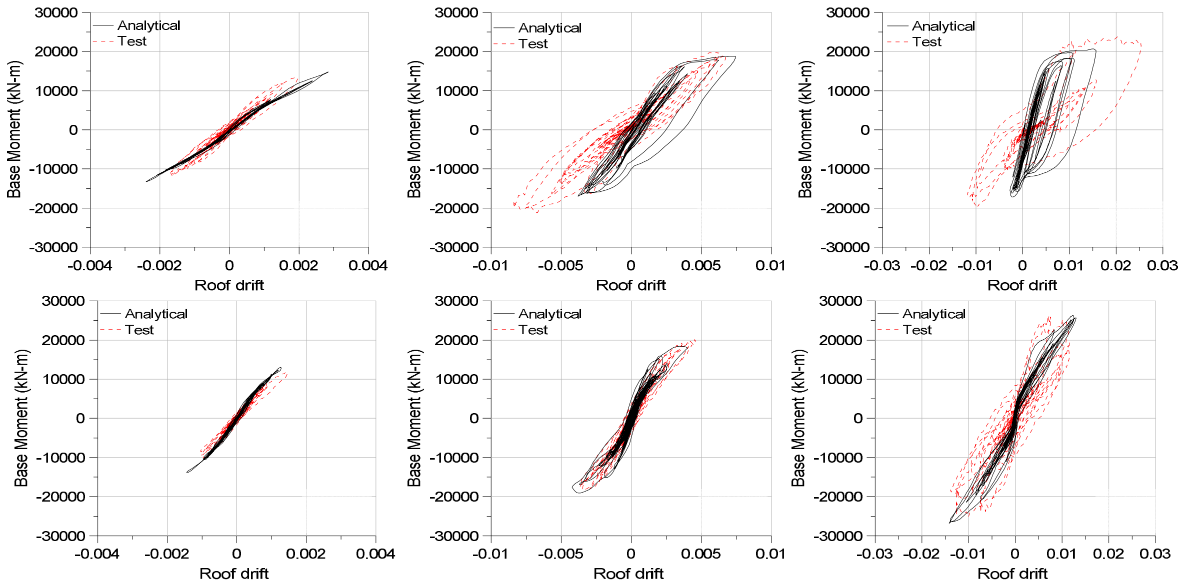

Figure 9. Comparison of analytical results with the test results at (a) 25%, (b) 50%, (c) 100% Kobe for the RC building; (d) 25%, (e) 50%, (f) 100% Kobe for the PT building

5. ENHANCED MODELING AND RESULTS OF THE RC BUILDING

Potential impact of reinforcing bar slip/extension was modeled explicitly in the RC model by adding nonlinear moment-rotation springs at the base and top of the columns, as well as at the beam-column interfaces. The contribution of slip/extension was estimated using the approach recommended by Alsiwat and Saatcioglu (1992), where cumulative displacements (bar extensions) were obtained by integrating the strains along the rebar development length (l_d), and then were divided by the neutral axis depth of the beam (or column) to achieve beam (or column) yield rotation (θ_y). Rotational springs were implemented in Perform 3D as tri-linear backbone curves in which strength deterioration was assumed to occur once the slip demand exceeds 3 mm (Lowes et al., 2004). Effective stiffness of the members was modified to be equal to $0.5EI_g$ and cyclic degradation was included, as recommended by Naish (2010). Slip/extension deformations in the walls were neglected as they generally do not contribute significantly. Wall sliding at the wall-foundation interface was modeled by adding translational springs between the wall base and the foundation (additional nodes were added to accomplish this). In the preliminary study reported here, sliding behavior was defined as elastic to understand the influence of sliding in the overall response. The effective stiffness for the sliding springs was estimated using the shear force vs. sliding displacement relationship obtained from the actual test data. Cyclic degradation was included in the reinforcing steel behavior as described by Orakcal et al. (2006), as well as in the beam moment-rotation hinges based on the recommendations by Naish et al. (2010). Additionally, tension behavior of concrete was included in the model with peak tensile capacity of $f_t = 7.5\sqrt{f_c^{'}}$ and post-peak stiffness of $E_t = 0.05E_c$ (Orakcal, 2004), where E_c is modulus of elasticity of concrete.

Comparisons of results based on base moment vs. roof drifts (Figure 10) indicate that including these modeling parameters significantly improved the correlation between model and test results. For all three records, the overall load-displacement relation is reasonably captured, although strength degradation and peak lateral displacement are modestly overestimated for the 100% Kobe record. Future studies will focus on refining the sliding models. A bilinear model could be used to account for the near rigid behavior prior to initiation of shear sliding (e.g. in 25% Kobe record). In addition, interpretation of the actual test data indicated that sliding stiffness significantly dropped once the concrete crushed and rebars buckled at the wall boundaries; however, Perform 3D is not capable of modeling sliding behavior that is coupled with wall bending behavior. Future studies may include using an alternative computational platform. Additional factors that might address the discrepancies were identified as: (i) the parameters used to model strength deterioration and cyclic degradation; and (ii) effects of biaxial responses and torsion (current modeling involves two-dimensional analysis for the shear wall direction; however, three-dimensional analysis is needed to investigate these issues.

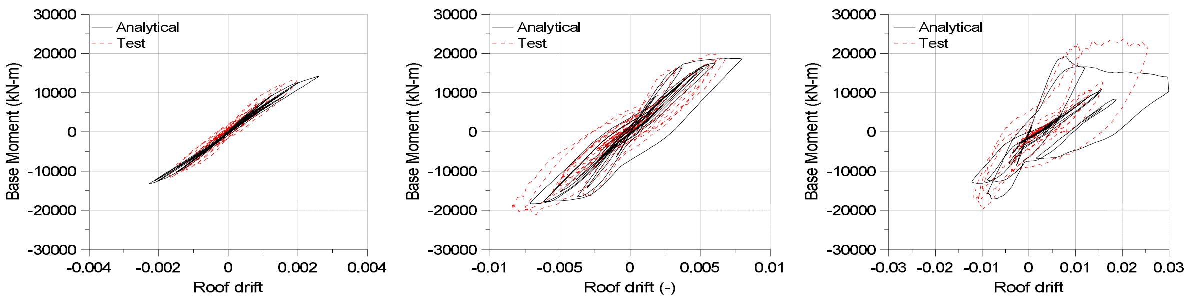

Figure 10: Comparison of analytical results with the test results at (a) 25%, (b) 50%, (c) 100% Kobe

6. CONCLUSIONS

Detailed modeling studies related to the December 2010 tests of two, full-scale, four-story buildings that were tested on the NIED E-Defense shake table are presented along with a brief summary of the tests. Ability of current nonlinear modeling techniques to capture the lateral load versus roof displacement relations were assessed by comparing experimental and analytical results. Analytical results for the RC building revealed that the preliminary (blind) model was capable of adequately capturing the responses at the service-level event. However, additional features such as slip/extension of longitudinal reinforcement, sliding-shear behavior at the wall-foundation interface, and cyclic degradation were included in the model to better capture responses at collapse-level events where significant strength loss and stiffness degradation were observed. Although the enhanced model substantially improved the global responses, some discrepancies were still observed for the 100% Kobe record. Future studies will focus on refining the sliding models, sensitivity of the parameters used to model strength degradation and cyclic degradation, and assessment of local responses. For the PT building it was found that a model consisting of inelastic fiber cross sections for UPT walls and elastic beam-column elements with gross section properties for prestressed beams and columns provided reasonably accurate predictions of the global response for the service level event. To capture the response at higher shaking intensities the nonlinear behavior at beam-column and beam-wall connections were modeled using beam moment-rotation hinges. Although overall satisfactory predictions of the global responses were obtained, some discrepancies were observed especially for the 100% Kobe record. Future studies will focus on refining the modeling of the gap-opening behavior at the beam-column and beam-wall connections (e.g., by using inelastic fiber sections or nonlinear elastic rotational springs), investigating damping associated with impact at the base of the wall and assessing local responses.

ACKNOWLEDGMENTS

Funding for US participation in this study was provided by U.S. National Science Foundation under award CMMI-1000268, whereas funding for NEES@UCLA instrumentation was provided under award CMMI-1110860. The authors would like to acknowledge Dr. A. Salamanca of the NEES@UCLA, Dr. S. Sritharan of Iowa State University, and Professor T. Kabeyasawa at the Earthquake Research Institute at the University of Tokyo for providing additional instrumentation for the test buildings. Opinions, findings, conclusions, and recommendations in this paper are those of the authors, and do not necessarily represent those of the sponsors or other individuals mentioned here.

REFERENCES

Alsiwat J. M., and Saatcioglu M. (1992). Reinforcement Anchorage Slip under Monotonic Loading. *J. Struct. Eng., ASCE*, **Vol.118**, No.9, Sept. 1992. pp. 2421-2438

Applied Technology Council. (2010). ATC-72: Modeling and Acceptance Criteria for Seismic Design and Analysis of Tall Buildings. ATC, Redwood City, CA.

ASCE/SEI Seismic Rehabilitation Standards Committee. (2007). Seismic Rehabilitation of Existing Buildings (ASCE/SEI 41-06),American Society of Civil Engineers, Reston, VA, US.

ASCE/SEI 7. (2010). Minimum Design Loads for Buildings and Other Structures, Structural Engineering Institute of the American Society of Civil Engineers.

Birely, A., Lehman, D., Lowes, L., Kuchma, D., Hart, C., and Marley, K. (2010). Investigation of the Seismic Response of Planar Concrete Walls. Proceedings Paper 773, *9th U.S. National Conference and 10th Canadian Conference on Earthquake Engineering*, Ontario, Canada, 2010.

Carr, A. J. (2010). Ruaumoko Program for Inelastic Dynamic Analysis, Users Manual, Department of Civil Engineering, University of Canterbury, Christchurch, New Zealand.

CSI Perform 3D V5. (2011). Nonlinear Analysis and Performance Assessment for 3D Structures. Computer and Structures, Inc. Berkeley, CA.

El Sheikh, M T., Sause, R., Pessiki, S., Lu, L.W., (1999). Seismic behavior and design of unbonded post-tensioned precast concrete frames. *PCI Journal*, 44(3), 54-71.

Elwood, K. J., Matamoros, A. B., Wallace, J. W., Lehman, D. E., Heintz, J. A., Mitchell, A. D., Moore, M. A., Valley, M. T., Lowes, L. N., Comartin, C. D., and Moehle, J. P. (2007).Update to ASCE/SEI 41 Concrete Provisions. *Earthquake Spectra*, **Vol. 23**, No. 3, pp. 493~523.

Holden, T., Restrepo, J., Mander, J.B. (2003). Seismic performance of precast reinforced and prestressed concrete walls. *J. Struct. Eng., ASCE*, **Vol.129**, No.3, pp. 286-296.

Kurama, Y.C., Sause, R., Pessiki, S., and Lu, L.-W. (1999). Lateral load behavior and seismic design of unbounded post-tensioned precast concrete walls. *ACI Structural Journal*, **96(4)**:622–632.

Lowes, L.N., Mitra, N., and Altoontash, A., (2004). A Beam-Column Joint Model for Simulating the Earthquake Response of Reinforced Concrete Frames. *PEER Report*, PEER 2003/10. Feb. 2004, UC Berkeley.

Ma, Q. T., Wight, G. D., Butterworth, J. W., & Ingham, J. M. (2006). Assessment of Current Procedures for Predicting the In-plane Behavior of Controlled Rocking Walls. *8th U.S. National Conference on Earthquake Engineering (8NCEE)*, April 18-22, San Francisco, California, U.S.A.

Naish, D. (2010). Testing and Modeling of Reinforced Concrete Coupling Beams. *Ph.D. Dissertation*. University of California, Los Angeles.

Nagae, T.; Wallace, J. W. (2011). Design and instrumentation of the 2010 E-Defense four-story reinforced concrete and post-tensioned concrete buildings*, PEER Report,* PEER-2011/104. June 2011, UC Berkeley.

Orakcal, K., Wallace, J. W. (2006). Flexural Modeling of reinforced Concrete Walls - Experimental Verification. *ACI Structural Journal,* **Vol. 103**, No. 2, March-April 2006.

Pampanin, S., Priestley, M.J.N. and Sritharan, S. (2001). Analytical Modelling of the Seismic Behaviour of Precast Concrete Frames Designed with Ductile Connections. *J. Earthquake. Eng.*, **Vol.5** No3, 329-367.

Panagiotou, M. (2008). Seismic design, testing and analysis of reinforced concrete wall buildings, *PhD Dissertation*, Dept. of Civil Engineering, University of California, San Diego, CA.

Pacific Earthquake Engineering Research Center, OpenSees - Open System for Earthquake Engineering Simulation, University of California, Berkeley, California, http://opensees.berkeley.edu.

Perez, F.J., Pessiki, S., and Sause, R. (2004). Experimental and analytical lateral load response of unbonded post-tensioned precast concrete walls, ATLSS Report No. 04-11, Lehigh University, Bethlehem, PA.

Razvi, S., and Saatcioglu, M. (1999). Confinement model for high-strength concrete. *J. Struct. Eng., ASCE,* **Vol.125** No.3, pp. 281-289.

Tuna, Z., (2009). Quantification of Seismic Performance Levels of Tall Buildings. *M.S. Thesis*. University of California, Los Angeles.